Biochimica et Biophysica Acta, 1110 (1992) 20–28

BBAMEM 75725

Determination of rate constants for nucleotide dissociation from Na,K-ATPase

Mikael Esmann

Institute of Biophysics, University of Aarhus, Aarhus (Denmark)

(Received 27 March 1992)

Key words: ATPase, Na^+/K^+-; Nucleotide dissociation; Rate constant

A method for determining individual rate constants for nucleotide binding to and dissociation from membrane bound pig kidney Na,K-ATPase is presented. The method involves determination of the rate of relaxation when Na,K-ATPase in the presence of eosin is mixed with ADP or ATP in a stopped-flow fluorescence apparatus. It is shown that the nucleotide dependence of this rate of relaxation – taken together with measured equilibrium binding values for eosin and ADP – makes possible a reasonably reliable determination of the rate constant for dissociation of nucleotide, i.e., determination of the rate constant k_{-1} in the following model (where E denotes Na,K-ATPase):

$$E \cdot Eosin \underset{[Eosin] \cdot k_2}{\overset{k_{-2}}{\rightleftharpoons}} E \underset{k_{-1}}{\overset{[ADP] \cdot k_1}{\rightleftharpoons}} E \cdot ADP$$

All experiments are carried out at about 4°C in a buffer containing 200 mM sucrose, 10 mM EDTA, 25 mM Tris and 73 mM NaCl (pH 7.4). Values obtained for the rate constants for dissociation are about 6 s^{-1} for ADP and 2–3 s^{-1} for ATP.

Introduction

The Na,K-ATPase is an integral membrane-bound cation transport enzyme, responsible for the active transport of Na^+ and K^+ across the plasma cell membrane (see Ref. 1 for a recent collection of reviews). The reaction mechanism of the enzyme involves binding of nucleotide (ATP) and cations, and transport of the cations is thought to involve a number of phosphorylated intermediates. An important step in the reaction sequence involves nucleotide binding to the enzyme, a step prior to phosphorylation. The Na,K-ATPase has one high-affinity nucleotide binding site per enzyme molecule, and dissociation constants are in the submicromolar range [2,3], as evidenced from a number of equilibrium binding studies. The individual rate constants for nucleotide binding (k_1, dimension $\mu M^{-1} s^{-1}$) and dissociation (k_{-1}, s^{-1}) are difficult to measure directly for ADP or ATP (see Ref. 4 for a discussion), whereas both rate constants have been determined directly from stopped-flow fluorescence experiments for the fluorescent nucleotide analogues FDP and FTP [5]. The fluorescent dye eosin has also been used to investigate the properties of ligand-induced changes in nucleotide affinity. This dye binds to the nucleotide site with a relatively high affinity [6] and the fluorescence of bound eosin is enhanced several-fold upon binding.

The purpose of the present investigation has been to demonstrate that the time-dependence of a perturbation of the enzyme · eosin complex, measured as a fluorescence change in a stopped-flow apparatus, can be used to determine the individual rate constants for nucleotide binding and dissociation. The dissociation constants for ADP and eosin are determined independently, and the interaction between eosin and ADP in equilibrium studies can be interpreted according to a simple model with the nucleotide binding site occupied either by ADP or by eosin. Individual rate constants for eosin binding and release under the present experimental conditions are determined from stopped-flow fluorescence experiments [6] and the influence of nu-

Correspondence to: M. Esmann, Institute of Biophysics, Ole Worms Allé 185, University of Aarhus, DK-8000 Aarhus, Denmark.

Abbreviations: E_1, the enzyme form predominant in the presence of Na^+; E, Na,K-ATPase; Eo, eosin; A, nucleotide (ADP or ATP); EEo, the Na,K-ATPase-eosin complex; EA, the Na,K-ATPase-nucleotide complex; k_{obs}, observed rate constant (from an exponential fit); K_{ns}, constant describing the non-specific binding of eosin; K_A, equilibrium dissociation constant for nucleotide; K_{Eo}, equilibrium dissociation constant for eosin.

cleotide concentrations on the observed rate of dissociation of eosin from the enzyme is interpreted in the simple model with rate constants for ADP dissociation and binding of 6 s^{-1} ($= k_{-1}$) and 31 $\mu M^{-1} s^{-1}$ ($= k_1$). The rate constant for ATP dissociation can in similar experiments be determined to be about 2–3 s^{-1}.

Methods and Materials

Preparation of pig kidney enzyme. Na,K-ATPase was isolated in the membrane bound form from pig kidney outer medulla by the method of Jørgensen [7] followed by selective extraction of the plasma membranes with SDS in the presence of ATP. The enzyme was stored at −20°C in 250 mM sucrose, 12.9 mM imidazole, and 0.625 mM EDTA at pH 7.5. The specific ouabain-inhibitable Na,K-ATPase activity varied between 1100 and 1600 μmol/mg protein per h at 37°C. Na,K-ATPase activity and protein content was determined as previously described [8].

Equilibrium ADP binding assay. ^{14}C-ADP binding was measured by a centrifugation assay as described by Nørby and Jensen [9]. Briefly, Na,K-ATPase membranes were suspended at 4°C in a buffer containing 200 mM sucrose, 10 mM EDTA, 25 mM Tris and 73 mM NaCl (pH 7.4) and varying amounts of ADP and eosin. Bound ADP was removed by centrifugation, and amounts of bound and free ADP determined. The enzyme was kept in the dark throughout the experiment.

Equilibrium fluorescence measurements. Equilibrium binding of eosin at 4°C was done as described earlier [6] using the centrifugation technique. Na,K-ATPase membranes were suspended at 4°C in a buffer containing 200 mM sucrose, 10 mM EDTA, 25 mM Tris and 73 mM NaCl (pH 7.4) and varying amounts of ADP and eosin. The concentration of free (unbound) eosin is determined, after pelleting of the membranes, from the eosin-fluorescence at 23°C in a Perkin-Elmer MPF 44A spectrofluorimeter. Excitation was at 530 nm, and emission was monitored at 560 nm (both slits being 10 nm).

Stopped-flow fluorimetry. Measurements of rates of changes in fluorescence were carried out with a SFM-2 stopped-flow apparatus (Biologics, France). Excitation was at 530 nm, and emission was measured with a photomultiplier with a cut-off filter at 550 nm. Data were collected with an A/D-converter interfaced to an HP 9816 microcomputer. The signal-to-noise ratio was increased by digitally adding 3–5 tracings. Non-least-squares calculation of exponential decays were performed using a programme kindly provided by Dr. Robert Clegg, Göttingen.

Samples were prepared in the following way: Both stopped-flow syringes contained a buffer with 200 mM sucrose, 10 mM EDTA, 25 mM Tris and 73 mM NaCl (pH 7.4) and varying amounts of ADP, ATP and eosin (see the legends to Figs. 3 and 6). In addition, one syringe contained Na,K-ATPase membranes (at a concentration of 0.1 mg/ml before mixing). The volume

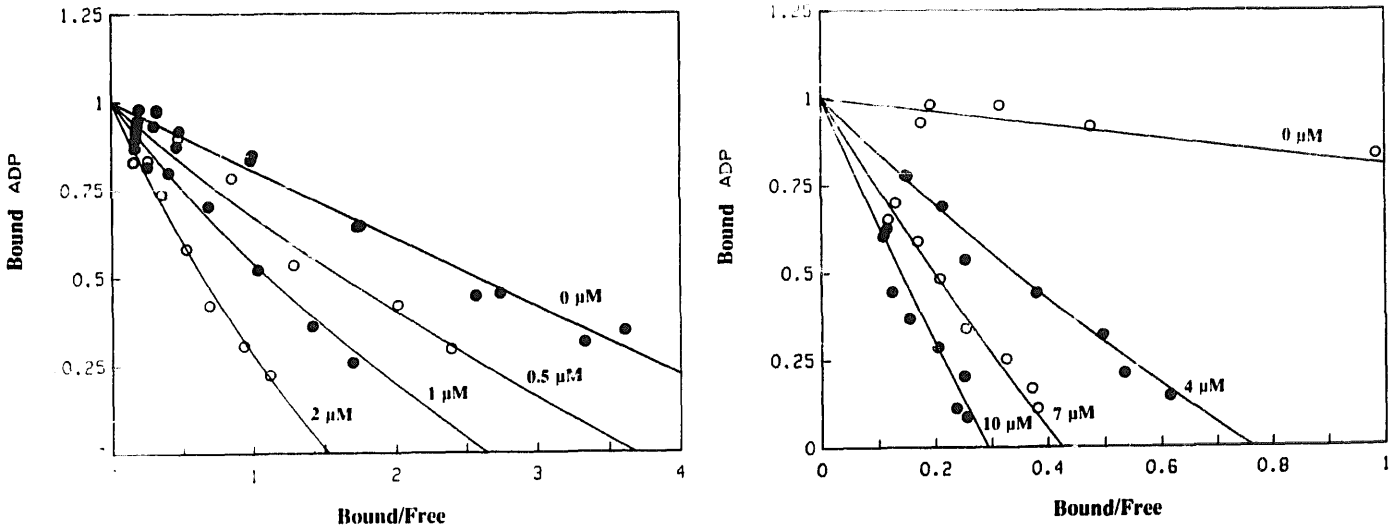

Fig. 1. Normalized Scatchard plots of ADP binding to Na,K-ATPase in the presence of various concentrations of eosin. The eosin-concentrations shown in the figure are the total concentrations of eosin, $[Eo]_{Tot}$, ranging from 0 to 2 μM (left) and from 4 to 10 μM (right, here is also shown the binding isotherm in the absence of eosin). The curves were simulated according to Eqn. 3 using the relations shown in Scheme I with $K_A = 0.195$ μM, $K_{Eo} = 0.4$ μM and a non-specific binding constant $K_{ns} = 1.0$ nmol eosin/mg protein per μM free eosin. The curves have been normalized to give an $[E]_{Tot} = 1.0$. This normalization was performed due to a slight variation in the intercept with the ordinate, notably a decrease in $[E]_{Tot}$ at high eosin-concentrations (see text). The experiment was done in a buffer containing 200 mM sucrose, 10 mM EDTA, 25 mM Tris and 73 mM NaCl (pH 7.4).

$$E + A \underset{k_{-1}}{\overset{k_1}{\rightleftharpoons}} EA \qquad K_A = \frac{[E]\cdot[A]}{[EA]} = \frac{k_{-1}}{k_1}$$

$$E + Eo \underset{k_{-2}}{\overset{k_2}{\rightleftharpoons}} EEo \qquad K_{Eo} = \frac{[E]\cdot[Eo]}{[EEo]} = \frac{k_{-2}}{k_2}$$

$$[E]_{Tot} = [E] + [EA] + [EEo]$$

$$[A]_{Tot} = [A] + [EA]$$

$$[Eo]_{Tot} = [Eo] + [EEo] + K_{ns}\cdot[Eo]$$

Differential equations for time-dependence calculations:

$$[E]_{t+dt} = [E]_t + \{[EA]_t\cdot k_{-1} + [EEo]_t\cdot k_{-2} - [E]_t\cdot(k_1\cdot[A]_t + k_2\cdot[Eo]_t)\}\cdot dt$$

$$[EA]_{t+dt} = [EA]_t + \{[E]_t\cdot k_1\cdot[A]_t - [EA]_t\cdot k_{-1}\}\cdot dt$$

$$[EEo]_{t+dt} = [EEo]_t + \{[E]_t\cdot k_2\cdot[Eo]_t - [EEo]_t\cdot k_{-2}\}\cdot dt$$

Scheme I.

delivered from each syringe was 150 μl per shot, the flow-time being 200 ms. This gives a dead time of about 2 ms in this apparatus, which is sufficiently short for the reactions to be followed in these experiments.

Materials. Eosin was obtained from Koch-Light.

Results

I. Effect of eosin on equilibrium binding of ADP

Fig. 1 shows the binding isotherms for ADP in the presence of eosin in concentrations between 0 and 10 μM. In the absence of eosin the isotherm is a straight line with a negative slope of 0.195, the value for the dissociation-constant for ADP (K_A, see Scheme I) under the present experimental conditions. Addition of eosin to the equilibrium-binding assay leads to an increase in the negative slope of the binding isotherms and also induces a curvature in the binding isotherms. Both effects of eosin can be accounted for with the model shown in Scheme I. Eosin here acts as a competitor for ADP, presumably by blocking the nucleotide binding site when the enzyme · eosin complex (EEo) is formed, this leads to the increase in the slope of the isotherms. Eosin also binds in a non-specific manner (see below) to the enzyme, which leads to the observed upward curvature of the isotherms. The lines in Figs. 1A and 1B are simulated according to the model shown in Scheme I with dissociation constants $K_A = 0.195$ μM for ADP and $K_{Eo} = 0.4$ μM for eosin, and allowing for a non-specific binding, which is proportional to the free eosin concentration: $K_{ns} = 1$ nmol eosin bound/mg protein per μM free eosin (this value for K_{ns} is obtained independently from binding of eosin, see Fig. 2 below). The non-linearity of the curves of bound versus bound/free nucleotide ([EA] versus [EA]/[A]) can be expressed in terms of the following equations:

$$[EA] = [E]_{Tot} - K_A\cdot[EA]/[A] - [Eo]\cdot K_A\cdot[EA]/(K_{Eo}\cdot[A]) \qquad (1)$$

and, since eosin has both specific and non-specific binding (see Scheme I)

$$[Eo]_{Tot} = [Eo] + [EEo] + K_{ns}\cdot[Eo] \qquad (2)$$

the concentration of bound nucleotide [EA] can be expressed in terms of [EA]/[A] (after re-arranging):

$$[EA] = [E]_{Tot} - \{[EA]\cdot K_A/[A]\}\cdot\{1 + [Eo]_{Tot}/(K_{Eo} + K_{ns}\cdot K_{Eo} + K_A\cdot[EA]/[A])\} \qquad (3)$$

Note that the binding isotherms have been normalized to $[E]_{Tot} = 1.0$. This was done firstly because different preparations with different specific Na,K-ATPase activities were used (the maximal binding capacity E_{Tot} varied between 1.9 and 2.7 nmol ADP binding sites/mg protein). A second reason for normalization was that at high eosin concentrations the maximal binding capacity for ADP (deduced from Scatchard plots) for a given enzyme preparation sometimes decreased compared to the value obtained in the absence of eosin. This is probably due to the irreversible denaturation of the enzyme by eosin, the rate of which is very light-sensitive (see Fig. 4 below).

II. Eosin interaction with Na,K-ATPase

Equilibrium measurements

Eosin binding can be determined from equilibrium centrifugation studies as previously described [6]. In addition to a specific binding of eosin (presumably to the nucleotide binding site), there is a non-specific binding of eosin to the Na,K-ATPase membranes, Fig. 2. Here is shown the binding of eosin in the presence of 73 mM NaCl in the absence or presence of 100 μM ADP. As previously observed, there is a linear dependence of the amount of eosin bound on the free eosin concentration, with a proportionality constant of about 1 nmol eosin bound/mg protein per μM free eosin ($= K_{ns}$). This is taken as non-specific binding of eosin to the Na,K-ATPase membranes. If ADP is omitted from the binding assay, there is as previously observed a saturable component of eosin binding in addition to the non-specific binding, with a half-maximal (specific) binding of eosin at about 0.34 μM free eosin, in agreement with the observations shown in Fig. 1 ($K_{Eo} = 0.4$ μM). In the presence of 73 mM KCl instead of NaCl a binding similar to the non-specific component is observed, both in the presence and absence of ADP, in agreement with the interpretation that specific

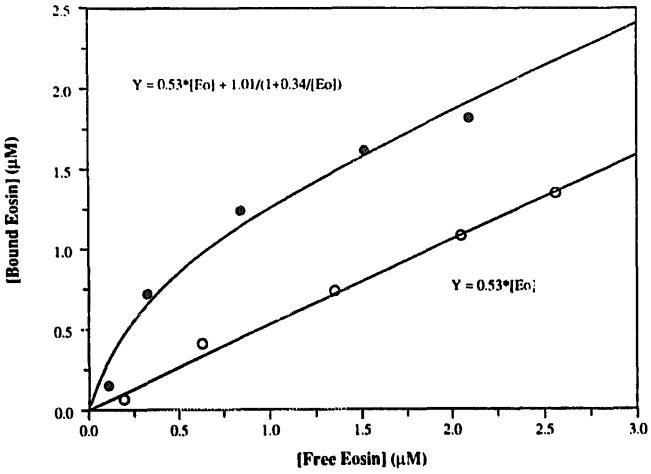

Fig. 2. ADP-sensitive eosin binding to Na,K-ATPase. The amount of eosin bound to the enzyme (0.49 mg protein/ml) is determined using the centrifugation technique. The binding (in the presence of 200 mM sucrose, 10 mM EDTA, 25 mM Tris and 73 mM NaCl (pH 7.4)) is shown as a function of the free eosin concentration in the absence of ADP (filled circles) and in the presence of 0.1 mM ADP (open circles). The binding in the presence of ADP is fitted by a straight line with a slope of 0.53 (giving a non-specific binding constant of about 1 nmol eosin/mg protein per μM free eosin), and the additional (specific) binding of eosin in the absence of ADP has a hyperbolic dependence of the eosin concentration: $[EEo] = [EEo]_{max}/(1+0.34/[Eo])$ with $[EEo]_{max} = 1.01$ μM and a dissociation constant $K_{Eo} = 0.34$ μM.

eosin-binding requires the enzyme to be in the E_1-form, which is induced by Na^+.

Transient kinetic measurements of eosin binding

The specific binding of eosin is associated with an increase in the fluorescence yield with the bound eosin having a fluorescence which is 3–4-fold higher than unbound eosin [6]. Stopped-flow fluorescence measurements allows determination of the rate-constants for binding and dissociation of eosin, Fig. 3 (see Ref. 10 for details). The fluorescence tracings (shown in Fig. 3A) are best fitted by a sum of two exponential func-

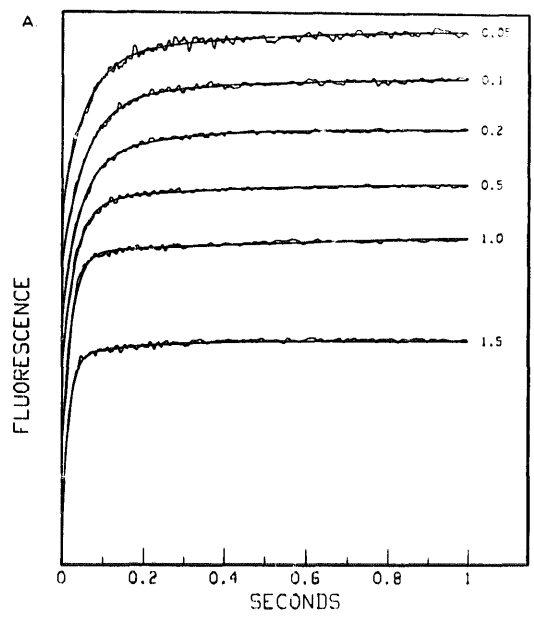

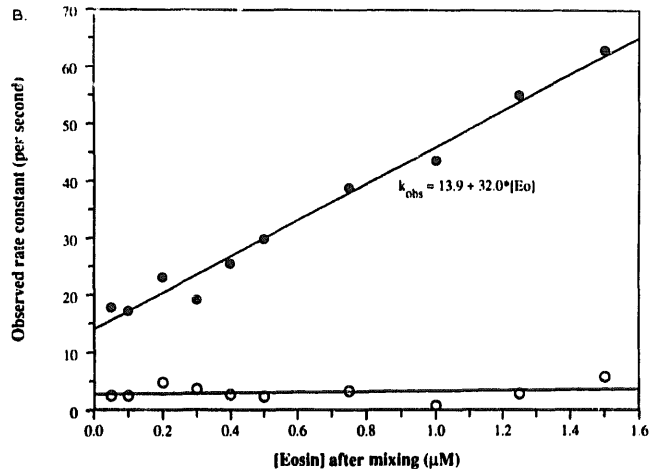

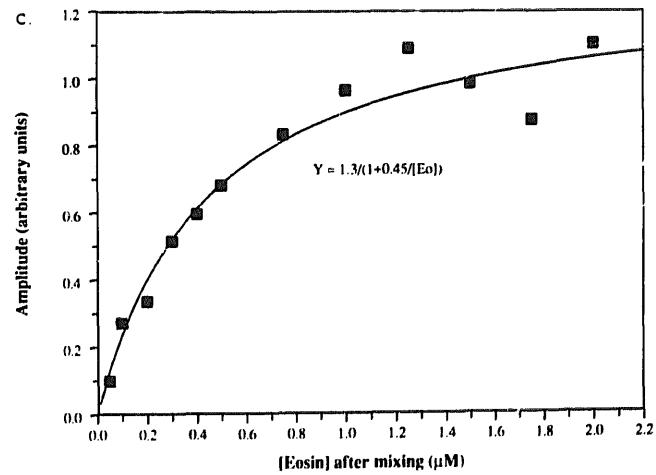

Fig. 3. Kinetics of eosin binding to Na,K-ATPase. Na,K-ATPase in buffer (200 mM sucrose, 10 mM EDTA, 25 mM Tris and 73 mM NaCl (pH 7.4)) is mixed with an equal volume of eosin in buffer, and the fluorescence increase is followed with time for 2 s (panel A) with the final eosin concentrations indicated on the figure (between 0.05 and 1.5 μM). The transients are fitted by a sum of two exponential terms, the observed rate constants of which are shown in panel B. The slow phase (observed rate constants represented by open circles) amounted to about 10% of the total increase in fluorescence signal. The continuous line through the data-points representing the majority (about 90%) of the fluorescence signal (filled circles) is a linear regression line $k_{obs} = k_2 \cdot [Eo] + k_{-2}$ with intercept 13.9 s^{-1} ($= k_{-2}$) and a slope of 32 μM^{-1} eosin per s ($= k_2$). Panel C shows the increase in the amplitude of the fluorescence signal as a function of the eosin concentration. The data points are fitted by a hyperbola of the form $Y = Y_{max}/(1 + K_{Eo}/[Eo])$ with $K_{Eo} = 0.45$ μM and $Y_{max} = 1.3$ (arbitrary units).

tions. In Fig. 3B is shown the concentration dependence of the observed rate constant for the increase in fluorescence when enzyme is mixed with eosin to give final concentrations between 0.05 and 1.5 μM eosin. The observed rate constant for the major (about 90%) part of the fluorescence change is linearly related to the eosin concentration as shown in Fig. 3B (filled circles). A minor component, which accounts for about 10% of the fluorescence change has an observed rate constant which is almost independent of the eosin concentration with a value of about 3 s^{-1}. The ratio between the intercept and the slope of the straight line for the major component (filled circles) gives the dissociation constant for eosin, which can be calculated to be about 13.9 $s^{-1}/32\ \mu M^{-1}s^{-1} = 0.43\ \mu$M (see the legend to Fig. 3 and Refs. 5, 6, 10 and 11 for details).

The total amplitude of the fluorescence change (Fig. 3A) as a function of the eosin concentration is shown in Fig. 3C. The data are adequately described by a hyperbolic function of the eosin concentration, with a half-maximal effect at 0.45 μM eosin, in good agreement both with the dissociation constant obtained from the binding experiments shown in Fig. 2, and with the dissociation constant deduced from the ratio between the individual rate constants (Fig. 3B), see Table I.

Light-sensitive denaturation of Na,K-ATPase by eosin

The Na,K-ATPase is irreversibly inactivated by eosin in low concentrations in the presence of visible light (from an ordinary light bulb), Fig. 4. Here the Na,K-ATPase activity is determined after incubation at 0°C with eosin concentrations between 0 and 50 μM. Note that the activity is reduced most rapidly at 2 to 5 μM

TABLE I

Kinetic constants for nucleotide and eosin binding to Na,K-ATPase

All experiments were done with pig kidney Na,K-ATPase in a buffer containing 200 mM sucrose, 10 mM EDTA, 25 mM Tris and 73 mM NaCl (pH 7.4) at about 4°C.

Equilibrium constants			
ADP			
K_A	equilibrium binding	Fig. 1	0.195 μM
Eosin			
K_{Eo}	displacement of ADP	Fig. 1	0.4 μM
K_{Eo}	equilibrium binding	Fig. 2	0.34 μM
K_{Eo}	fluorescence change	Fig. 3B	0.45 μM
Binding and dissociation rate constants			
ADP			
k_{-1}	displacement of eosin	Fig. 7A	6 s^{-1}
k_1	calculated from k_{-1} and K_A		31 $\mu M^{-1}s^{-1}$
ATP			
k_{-1}	displacement of eosin	Fig. 7B	2.5 s^{-1}
Eosin			
k_2	concentration jump	Fig. 3	32 $\mu M^{-1}s^{-1}$
k_{-2}	concentration jump	Fig. 3	14 s^{-1}

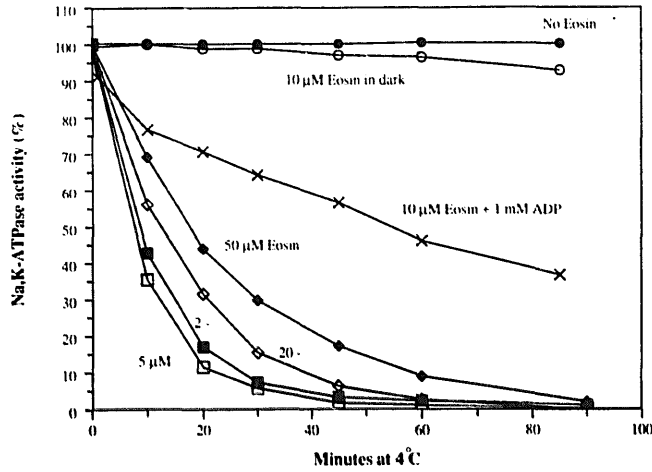

Fig. 4. Inactivation of Na,K-ATPase activity by eosin. Na,K-ATPase is incubated at 0°C about 20 cm below an ordinary 60W light bulb with the indicated concentrations of eosin in 2 ml buffer (200 mM sucrose, 10 mM EDTA, 25 mM Tris and 73 mM NaCl (pH 7.4)). After the time intervals shown an aliquot is diluted 100-fold into Na,K-ATPase assay medium and the residual activity is determined (at 37°C under standard conditions, Ref. 8). Data are shown in percent of the activity before the incubation at 0°C started. The following experimental conditions were tested: no eosin added (filled circles); eosin added to final concentrations of 2 μM (blocks), 5 μM (open squares), 20 μM (open diamonds) and 50 μM (filled diamonds); 10 μM eosin added, but the sample kept in the dark (open circles); 10 μM eosin added together with 1 mM ADP (crosses).

eosin, whereas higher concentrations (20–50 μM) protect the enzyme against inactivation. Inactivation is also slowed considerably by addition of ADP (crosses) or by protection from light (open circles). The double effect of eosin – inactivation at low concentration and protection at higher concentrations – can be explained if it is assumed that eosin has to bind to the specific binding site (K_{Eo} about 0.4 μM) before the light-induced inactivation takes place. A high concentration of eosin (20–50 μM) quenches the inactivation reaction, presumably due to absorption of light in the bulk phase (note that with an absorption coefficient $\epsilon = 8 \cdot 10^4\ M^{-1}cm^{-1}$ for eosin [12] there is an appreciable absorption of light at 50 μM eosin). The experiments clearly show the importance of keeping the enzyme in the dark in the presence of eosin. Even in the dark there is a slow enzyme-denaturation at 10 μM eosin, which can explain the small variation in the maximal ADP-binding capacity at high eosin concentrations (see above). The light-induced denaturation is much more rapid at higher temperatures (not shown).

III. Transient kinetics of interaction of ADP and eosin with the Na,K-ATPase

Simulation of transient changes in eosin fluorescence with different nucleotide concentrations

Fig. 5 shows a set of computer-simulated stopped-flow experiments of the fluorescence of eosin, simu-

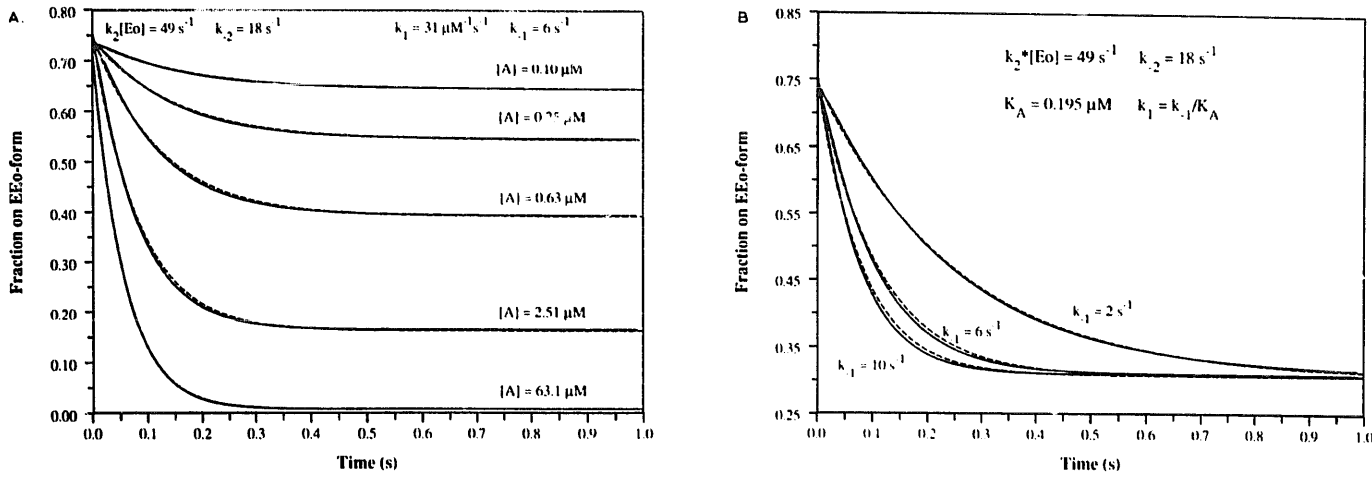

Fig. 5. Simulation of eosin fluorescence after addition of ADP. This figure shows the time dependence of the concentration of enzyme on the EEo-form on the rate constants assigned to the interconversion between the enzyme forms shown in Scheme I. Panel A shows a simulation of the time course of disappearance of EEo with the rate constants $k_2 = 45\ \mu M^{-1}s^{-1}$, $k_{-2} = 18\ s^{-1}$, $k_1 = 31\ \mu M^{-1}s^{-1}$, $k_{-1} = 6\ s^{-1}$, [Eo] = 1.1 μM and [A] taking values between 0.1 and 63 μM, using the differential equations shown in Scheme I. Panel B shows a set of simulations where $[EEo]_t$ is calculated with values $k_2 = 45\ \mu M^{-1}s^{-1}$, [Eo] = 1.1 μM, $k_{-2} = 18\ s^{-1}$, [A] = 1 μM and the ratio k_{-1}/k_1 kept constant 0.195 μM ($= K_A$), but allowing k_{-1} to obtain values of 2, 6 or 10 s^{-1}, i.e., the rate of relaxation at the ADP-binding step is increased.

lated according to the model shown in Scheme I, using the differential equations for the time-dependence of the enzyme species also shown in Scheme I. In these simulations the enzyme is allowed to be in equilibrium with eosin, and at time zero nucleotide is added at different concentrations. The rate constants for eosin binding and dissociation are here taken to be 45 $\mu M^{-1}s^{-1}$ (k_2) and 18 s^{-1} (k_{-2}) and an eosin concentration of 1.1 μM is assumed in this simulation. In panel A the rate-constant for dissociation of nucleotide (k_{-1}) is taken to be 6 s^{-1} and the association rate constant $k_1 = 31\ \mu M^{-1}s^{-1}$ (giving $K_A = 0.195\ \mu M$). There is a large increase in both rate and magnitude of the eosin fluorescence decrease when nucleotide is added in increasing concentrations ([A] is increased from 0.1 to 63 μM). Panel B shows a similar simulation

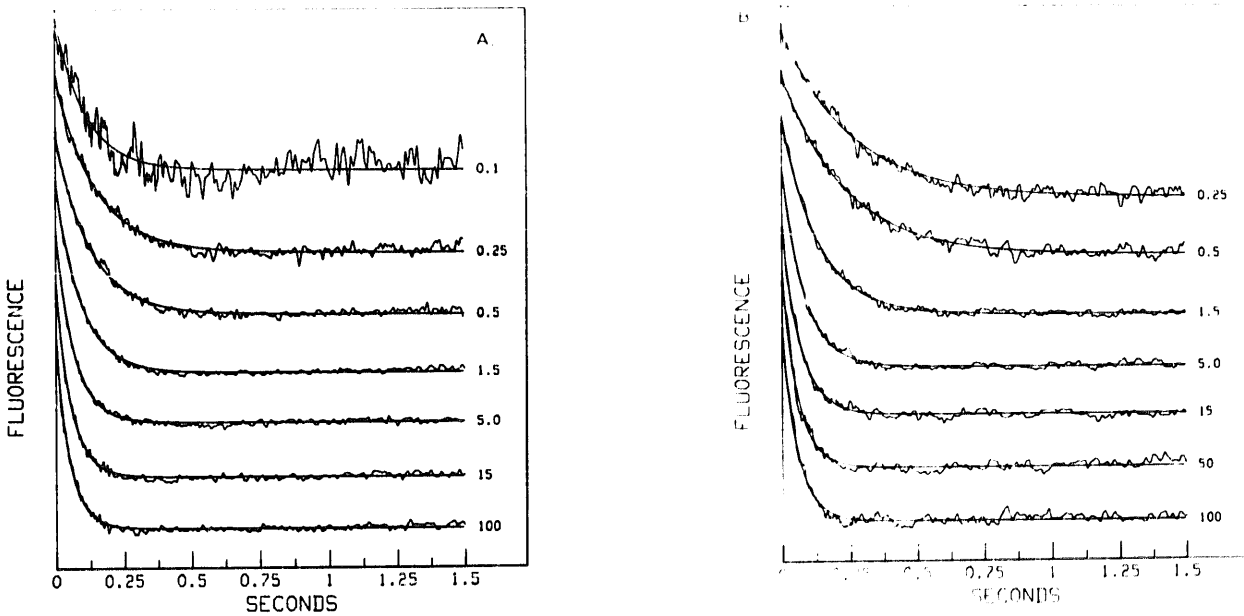

Fig. 6. Stopped-flow transients of eosin fluorescence induced by addition of nucleotides. Na,K-ATPase in buffer (200 mM sucrose, 10 mM EDTA, 25 mM Tris and 73 mM NaCl (pH 7.4)) with 1.1 μM eosin present is mixed with ADP (panel A) or ATP (panel B) in increasing amounts, giving final nucleotide concentrations between 0.1 and 100 μM. The time course of the fluorescence decay is shown, together with single-exponential fits of the transients. The transients have been normalized to about the same amplitude to ease comparison of the rate of change. The obtained values for the observed rate constants of the single-exponential fits are shown in Fig. 7.

at a given nucleotide concentration ([A] = 1 μM), but here k_1 and k_{-1} are varied (keeping the ratio $k_{-1}/k_1 = K_A = 0.195$ μM). The magnitude of k_{-1} is increased by a factor of 5 (from 2 to 10 s^{-1} tor k_{-1}, and thus about 10 to 51 for k_1). Clearly there is a more rapid decrease in fluorescence when the nucleotide binding- and dissociation-steps are allowed to be rapid. The simulated curves in Figs. 5A and 5B are fitted by single exponentials (dotted lines). The single-exponential fit seems to be an adequate description of the data (the dotted lines are almost all within the full lines of the simulations), although there is a small lag period in the simulated curves.

The result of the simulations in Fig. 5 forms the basis for the following experiments: since we can determine k_{-1}/k_1 ($=K_A$, the dissociation constant for ADP) accurately from equilibrium binding experiments (Fig. 1) and perform stopped-flow experiments in the same experimental range as shown in Panel A (Fig. 5), it is possible to estimate the individual values of k_{-1} and k_1.

Stopped-flow experiments of eosin fluorescence with increasing nucleotide concentrations

Fig. 6 shows a set of transient fluorescence tracings when Na,K-ATPase in the presence of 1.1 μM eosin is mixed with ADP (panel A) or ATP (panel B) to give final nucleotide concentrations between 0.1 and 100 μM. Note that the curves have been normalized to the same amplitude to ease comparison of the rate of changes. The real amplitude of the signal (not shown) increases with the nucleotide concentration in the same manner as is shown on the (simulated) transients in Fig. 5A. The transients shown in Fig. 6 are fitted by single exponentials as indicated in the figure, and the observed rate constants are shown as a function of the nucleotide concentration in Fig. 7. At high nucleotide concentrations there is a limiting observed rate constant of about 18 s^{-1} for both ADP (panel A) and ATP (panel B), and at low concentrations the value for the observed rate constant approaches about 6 s^{-1} for ADP and about 3 s^{-1} for ATP.

The nucleotide-concentration dependence of the observed rate constant for a single-exponential fit of simulated stopped-flow curves – such as those shown in Fig. 5A – are also shown in Fig. 7A. The curve indicated by a full line was simulated with $k_{-1} = 6$ s^{-1}, $k_1 = 31$ $\mu M^{-1} s^{-1}$, $k_{-2} = 18$ s^{-1} and $k_2 = 45$ $\mu M^{-1} s^{-1}$, which seems an adequate fit of the data (note that $K_A = 0.195$ μM and $K_{1/2} = 0.4$ μM). Similar simulations with the same values for eosin binding and dissociation and for K_A, but with k_{-1} taking a value of either 2 or 10 s^{-1}, are also shown (dotted lines).

Note that at high nucleotide concentrations the observed (simulated) rate constant approaches that of the dissociation rate constant for eosin (k_{-2}) and at very low nucleotide concentrations there is a marked decrease in observed rate constant – the value for k_{obs} approaches that of k_{-1}. The simulations clearly show the sensitivity of k_{obs} to k_{-1}, and allows for a reasonably accurate determination of k_{-1} – simply the limiting value at low nucleotide concentrations. The value used for k_{-2} (18 s^{-1}) is slightly higher than the value determined from eosin binding and dissociation (Fig.

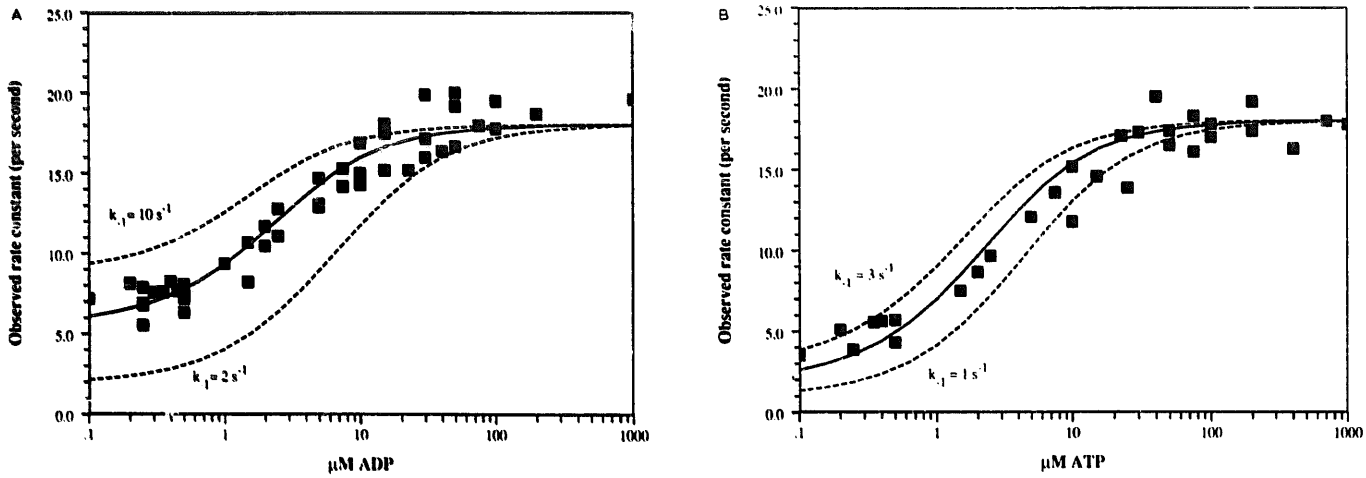

Fig. 7. The relationship between the observed rate constant for fluorescence decay and the nucleotide concentration. The observed rate constants of single-exponential fits such as those shown in Fig. 6 are plotted as a function of the final ADP (Panel A) or ATP concentration (Panel B) on a logarithmic scale. In panel A, the full line represents a computer simulation of the observed rate constants, simulated using rate constants for ADP of $k_1 = 31$ $\mu M^{-1} s^{-1}$ and $k_{-1} = 6$ s^{-1}, and for eosin of $k_2 = 45$ $\mu M^{-1} s^{-1}$ and $k_{-2} = 18$ s^{-1} with 1.1 μM eosin. The broken lines represent similar simulations with k_{-1} taken to be 10 s^{-1} (upper broken line) or 2 s^{-1} (lower broken line), with the ratio k_{-1}/k_1 kept constant at 0.195 μM ($= K_A$). In panel B, the full line shows the ATP-concentration dependence of the observed rate constant simulated in the same manner as for panel A, but with the rate constants $k_{-1} = 2$ s^{-1} and $k_1 = 31$ $\mu M^{-1} s^{-1}$ (giving $K_A = 0.065$ μM for ATP). The dotted lines show the relationship between the ATP-concentration and k_{obs} calculated for $k_{-1} = 1$ s^{-1} (lower dotted line) or $k_{-1} = 3$ s^{-1} (upper dotted line), keeping the dissociation constant $K_A = k_{-1}/k_1 = 0.065$ μM.

3). With a dissociation constant $K_{Eo} = 0.4\ \mu M$ we therefore have to use $k_2 = 45\ \mu M^{-1} s^{-1}$. This problem will be discussed below.

Discussion

Applicability of the method

The present paper introduces a method for determining individual rate constants for nucleotide binding to and release from Na,K-ATPase. The method relies on the ability of ADP (or ATP) to displace the fluorescent 'nucleotide analogue' eosin from the nucleotide binding site. In principle any probe which binds to the nucleotide site can be used, provided both that a spectroscopic property of the probe changes upon binding and that the change can be followed with a time-resolution in the appropriate range – here the decrease of the fluorescence yield of eosin upon dissociation is used in conjunction with stopped-flow fluorimetry. Other possible probes which could be used include the formycin-nucleotides FDP and FTP [5].

The method requires knowledge of the equilibrium constants for dissociation of ADP and eosin (K_A and K_{Eo}) together with the rate constants for eosin binding and dissociation. The equilibrium constant for ADP can be determined with great accuracy due to the high affinity for ADP ($K_A = 0.195\ \mu M$) and the absence of non-specific binding of ADP (Fig. 1). The value obtained in the present experiments compare favorably with the published values of 0.1–0.2 μM [2,3,12]. For eosin, the similar experiment is more complicated due to both the presence of a non-specific binding component and due to possible irreversible inactivation of the enzyme by eosin (Figs. 2 and 4). Comparison of the value for K_{Eo} (Table I) obtained from experiments on three different properties of eosin interaction (equilibrium binding (Fig. 2), amplitude of fluorescence response upon specific eosin binding (Fig. 3C) and ratio between dissociation and binding rate constants (Fig. 3B) gives values between 0.34 and 0.45 μM, which compares favorably to $K_{Eo} = 0.45\ \mu M$ previously found for shark rectal gland Na,K-ATPase.

Comparison of the simple model with the experiments

A single-exponential analysis of the fluorescence tracings from the stopped-flow experiments (Fig. 6 and 7) has been used in the present paper. This analysis ignores a small lag-period before the onset of fluorescence decrease, which can be seen in simulations of the model shown in Scheme I (Fig. 5). The error in this way of analyzing the data is presumably small, especially since the stopped-flow tracings can easily be presented in such a manner that a lag period is (more or less) predominant, due to the nature of the stopped-flow experiment (it is difficult to distinguish the last milliseconds of the 'flow' period from a small lag-period after the flow has been stopped, see Ref. 13 for a discussion). The closeness of exponential fit to the simulated curves in Fig. 5 also suggest that the single-exponential analysis (Fig. 6) is adequate for the results sought with the present experiments. Simple algorithms for a personal computer for simulating the curves shown in Figs. 1 and 5 can be provided by the author upon request.

Relaxation theory in relation to the stopped-flow experiments

The relaxation when the concentration of a ligand such as ADP is changed (cf. the system shown in Scheme I) can be expressed as an observed rate constant provided the changes in concentration of the species E, EA and EEo are small (i.e., according to perturbation theory, see for example Refs. 11 and 14). The expression relating k_{obs} to the individual rate constants appropriate for the system shown here is

$$k_{obs} = 0.5 \cdot \left[k_1 \cdot [A] + k_{-1} + k_2 \cdot [Eo] + k_{-2} \right. \\ \pm \left[(k_1 \cdot [A] + k_{-1} + k_2 \cdot [Eo] + k_{-2})^2 \right. \\ \left. \left. - 4 \cdot (k_{-1} \cdot k_{-2} + k_1 \cdot [A] \cdot k_{-2} + k_{-1} \cdot k_2 \cdot [Eo]) \right]^{1/2} \right] \quad (4)$$

As [A] approaches zero k_{obs} will approach k_{-1}, and for very large [A], k_{obs} will approach k_{-2} (taking the root with the negative sign). The dependence of k_{obs} (calculated according to equation 4) on the nucleotide concentration has a close similarity (not shown) to the fit obtained from simulation of the stopped-flow curves (full line in Fig. 7A), with the 'boundary conditions' of k_{obs} approaching k_{-1} (for [A] small) and k_{-2} (for [A] large) being met (see Fig. 7A). Small deviations can be explained either by the error in fitting a single exponential to curves which have a small lag period (most clearly seen at low [A], Fig. 5A or Fig. 6) or by the fact that the experiments performed here do not obey the criterion of 'small perturbations'. The latter circumstance – that there are very large changes in the concentrations of the individual enzyme species – is the reason that relaxation theory has not been used to characterize the present experiments in detail.

Bi-exponentiality of the fluorescence increase associated with eosin binding

Fig. 3A and 3B show that the fluorescence increase upon eosin binding is not single-exponential, but rather a sum of two exponential terms. The term with the major amplitude has an observed rate constant which is proportional to the eosin concentration, which is as should be expected from a model with a single eosin binding site (Scheme I). The minor component (about 10% of the total response, independent of the eosin

concentration) has a rate constant which is weakly (or not) dependent on the eosin concentration (Fig. 3B). In our earlier experiments with shark enzyme this component was not identified, probably due to the much lower signal/noise ratio in the early experiments [6]. There is no simple explanation for this small component. It has been observed that mixing of eosin with enzyme in the presence of ADP (to abolish specific eosin binding) also gives rise to a slow fluorescence increase, which could account for at least part of the small component seen in Fig. 3B. It is therefore conceivable that part of the small component is related to non-specific binding of eosin. Another possibility is that the fluorescence increase is not related simply to eosin binding in an all-or-none process as shown in Scheme I, but rather that the binding – and the increase in fluorescence yield – takes place in two or more steps, only one of which has an observed rate constant which is proportional to the eosin concentration. At present there is also no explanation for the finding that the rate-constant for eosin dissociation at high ADP-concentrations is 20–30% larger than the value of $k_{-2} = 13.9\ s^{-1}$ found from eosin binding experiments (Fig. 3B). Whether this is due to the above mentioned bi-exponentiality of the eosin-binding or to an enhancement of the rate of eosin dissociation by ADP can not be distinguished at present. A value of about 18 s^{-1} for k_{-2} was used in the model for the fitting of the data shown in Fig. 7, and k_2 (the on-rate constant for eosin) was taken to be 45 $\mu M^{-1} s^{-1}$, in order to keep the dissociation constant $K_{Eo} = 0.4\ \mu M$.

Comparison of the dissociation rate constants for ADP and ATP with other experiments

The problem of determining the value of the dissociation rate constant for ADP or ATP has been discussed previously in detail by Klodos and Nørby (see Table III in Ref. 4). The absolute values for the constants will probably depend very much on the experimental conditions, such as ionic strength, pH and temperature. The values obtained here for k_{-1} (about 6 s^{-1} for ADP and about 3 s^{-1} for ATP) are in good agreement with estimates from exchange reactions at 0°C, where values in the range 1.5–3.5 s^{-1} are found for ATP [4]. The binding rate constants for the nucleotides are in the present paper about 30 $\mu M^{-1} s^{-1}$, which compares favorably with estimates from stopped-flow experiments [5,6] and exchange reactions [4,15,16], which all are in the range of 10–40 $\mu M^{-1} s^{-1}$ (in the present study the dissociation constant for ATP has not been measured, but is assumed to be 3-fold smaller than that for ADP (see Ref. 9)). It is commonly assumed that the binding rate constants are diffusion-controlled (see Refs. 11, 17 and 18) which explains the similarity between found values for k_1 for ADP and eosin (this paper and Ref. 6) and for FDP and FTP [5]. The large difference between the dissociation rate constant k_{-1} for ADP (about 6 s^{-1}) and FDP or FTP (about 112 or 33 s^{-1}, respectively [5]) thus reflects the larger affinity for ADP than for FDP or FTP.

Conclusion

In conclusion, the advantage of the present method over earlier attempts to estimate the individual rate constants is that a very simple model for interaction between only two ligands and the enzyme is assumed (Scheme I), and the model is fully determined in terms of rate constants and equilibrium constants.

Acknowledgments

The author wishes to thank Ms. Birthe Bjerring Jensen and Ms. Angielina Tepper for excellent technical assistance, Dr. Jørgen Jensen and Jens G. Nørby for advice with the nucleotide equilibrium binding experiments and Dr. Igor Plesner for a critical reading of the manuscript. Financial support was received from the Danish Medical Research Council (Grant No. 12-8245), Aarhus University Research Foundation and from the Danish Biomembrane Research Center.

References

1 Kaplan, J.H. and De Weer, P. (eds.) (1990) The Sodium Pump, Society of General Physiologists Series, Vol. 46, Rockefeller University Press, New York.
2 Hegyvary, C. and Post, R.L. (1971) J. Biol. Chem. 246, 5234–5240.
3 Nørby, J.G. and Jensen, J. (1971) Biochim. Biophys. Acta 233, 104–116.
4 Klodos, I. and Nørby, J.G. (1987) Biochim. Biophys. Acta 897, 302–314.
5 Karlish, S.J.D., Yates, D.W. and Glynn, I.M. (1978) Biochim. Biophys. Acta 525, 230–251.
6 Skou, J.C. and Esmann, M. (1981) Biochim. Biophys. Acta 647, 232–240.
7 Jørgensen, P.L. (1974) Biochim. Biophys. Acta 356, 36–52.
8 Esmann, M. (1988) Methods Enzymol. 156, 105–115.
9 Nørby, J.G. and Jensen, J. (1988) Methods Enzymol. 156, 191–210.
10 Skou, J.C. and Esmann, M. (1983) Biochim. Biophys. Acta 746, 101–113.
11 Gutfreund, H. (1972) Enzymes: Physical Principles, Wiley Interscience, London.
12 Chan, S.S., Arndt-Jovin, D.J. and Jovin, T.M. (1977) J. Histochem. Cytochem. 27, 56–64.
13 Gibson, Q.H. (1969) Methods Enzymol. 16, 187–228.
14 Matsen, F.A. and Franklin, J.L. (1950) J. Am. Chem. Soc. 72, 3337–3341.
15 Mårdh, S. and Post, R.L. (1977) J. Biol. Chem. 252, 633–638.
16 Froehlich, J.P., Hobbs, A.S. and Albers, R.W. (1983) Curr. Top. Membr. Transp. 19, 513–535.
17 Hammes, G.G. and Schimmel, P.R. (1970) in The Enzymes (Boyer, P.D., ed.), Vol. 2, pp. 67–114, Academic Press, New York.
18 Hague, D.N. (1971) Fast Reactions, pp. 135–142, Wiley Interscience, London.